Sensors and Actuators B 233 (2016) 599–606

Contents lists available at ScienceDirect

Sensors and Actuators B: Chemical

journal homepage: www.elsevier.com/locate/snb

An electrochemical sensor based on molecularly imprinted polypyrrole/graphene quantum dots composite for detection of bisphenol A in water samples

Feng Tan*, Longchao Cong, Xiaona Li, Qian Zhao, Hongxia Zhao, Xie Quan, Jingwen Chen

Key Laboratory of Industrial Ecology and Environmental Engineering (MOE), School of Environmental Science & Technology, Dalian University of Technology, Dalian 116024, China

ARTICLE INFO

Article history:
Received 1 November 2015
Received in revised form 19 April 2016
Accepted 25 April 2016
Available online 27 April 2016

Keywords:
Bisphenol A
Electrochemical detection
Molecularly imprinted polymer
Graphene quantum dots

ABSTRACT

Bisphenol A (BPA) is an important endocrine disrupter in environments, for which sensitive and selective detection methods are highly necessary to carry out its recognition and quantification. Here a novel electrochemical sensor was developed based on molecularly imprinted polypyrrole/graphene quantum dots (MIPPy/GQDs) composite for the detection of bisphenol A (BPA) in water samples. A MIPPy/GQDs composite layer was prepared by the electropolymerization of pyrrole on a glassy carbon electrode with BPA as a template. The MIPPy/GQDs composite could specifically recognize BPA in aqueous solutions, which resulted in the decrease of peak currents of $K_3[Fe(CN)_6]$ at the MIPPy/GQDs) modified electrode in cyclic voltammetry (CV) and differential pulse voltammetry (DPV). There was a linear relationship between BPA concentrations ranging from 0.1 μM to 50 μM and the response value (ΔI_{DPV}) in DPV, with a limit of detection of 0.04 μM (S/N = 3). The sensor was applied for the detection of BPA in tap and sea water samples, with recoveries of 94.5% and 93.7%, respectively. The proposed method provides a powerful tool for rapid and sensitive detection of BPA in environmental samples.

1. Introduction

Bisphenol A (2,2-bis (4-hydroxyphenyl) propane, BPA) is an endocrine disrupter in environments, which can induce abnormal differentiation of reproductive organs by interfering the action of endogenous gonadal steroid hormones [1]. Low–dose exposure to BPA produces an increasing risk suffering from diabetes mellitus and cardiovascular disease [2]. Many researches showed that BPA has been found in daily plastics products such as nursing bottles, resin lining of cans, drinking water bottles, medical apparatus, and food packaging bags, etc., which results in potential risks to public health, especially for newborn infants and children. Hence, there is a great need to develop reliable analytical methods for sensitive detection of trace BPA in the fields of environmental monitoring, food safety and toxicity assessment.

The traditional techniques for BPA detection mainly include high performance liquid chromatography (HPLC) [3,4], high performance liquid chromatography–mass spectrometry (HPLC–MS and HPLC–MS/MS) [5–7], gas chromatography–mass spectrometry (GC–MS) [8,9]. Although these methods are reliable and sensitive enough for routine analysis, there are several shortcomings to be addressed, such as the needs for expensive equipment, well-trained operators and complicated sample preparation, and not being competent for on-site detection in emergent pollution events.

Electrochemical (EC) method is alternative for the detection of BPA [10–13]. However, direct EC detection for BPA suffered from several problems. The first problem is that there is an high overpotential in the oxidation of phenolic hydroxyl group of BPA at traditional electrodes [14,15], which results in an increase of background current and then a high limit of detection. The other problem is that the oxidized products of BPA easily attach, even form a thin film on sensing electrodes, which leads to passivation of the electrodes and thus a decreasing sensitivity in successive measurements [14,16].

Recently, several indirect EC methods which do not involve in the oxidation of the phenolic hydroxyl group have been reported for the detection of BPA, such as potentiometric [17,18], capacitive [19], impedimetric [20–22] sensors. These methods used specific recognition molecules/materials as electrode sensing elements, including molecularly imprinted polymer (MIP) [17], antibodies [18,20], tyrosinase [21], and DAN aptamer [19]. Selective binding or absorption of BPA on the sensing elements led to changes of potential, capacitance, or impedance in the sensing electrodes,

* Corresponding author at: School of Environmental Science and Technology, Dalian University of Technology, Linggong Road 2, Dalian 116024, China.
E-mail address: tanf@dlut.edu.cn (F. Tan).

http://dx.doi.org/10.1016/j.snb.2016.04.146
0925-4005/

which was used as response signal for quantifying BPA. Among these molecules/materials, MIP has many advantages, such as low preparation cost, ease of synthesis, and good chemical/mechanical stability in environments.

Graphene has attracted increasing attentions due to its' unique nanostructure and properties. Especially, large surface area, fast electron transfer rate, excellent electrical conductivity allow graphene as sensing element in EC detections [23]. On the other hand, strong hydrophobic nature is disadvantageous for the redox of analytes at grapheneinterface in aqueous solutions due to interface resistance. Graphene quantum dots (GQDs) are graphene sheets whose size is less than 100 nm. Besides the unique properties of graphene, GQDs have excellent photoluminescence, good water solubility, and biocompatibility, and thus have been gained many applications in optical sensing platforms and bioimaging [24,25]. However, there are seldom reports using GQDs as sensing materials in EC detections [26,27].

In the present work, a novel electrochemical sensor based on molecularly imprinted polypyrrole/graphene quantum dots (MIPPy/GQDs) composite was developed for the detection of BPA in waters through differential pulse voltammetry (DPV), with $K_3[Fe(CN)_6]$ as an electrochemical probe. The detection do not involve oxidation of BPA at the composite electrode. The proposed sensor showed high sensitivity, good reproducibility, and stability. Furthermore, the proposed method was successfully applied for the detection of BPA in sea water and tap water, with satisfactory recoveries.

2. Experimental

2.1. Materials and apparatus

Graphene oxide flake was purchased from Nanjing XFNANO Materials Tech. Co. Ltd (Nanjing, China). Pyrrole (99%) was purchased from Sigma–Aldrich (St. Louis, USA), which was further purified by vacuum distillation. Bisphenol A (BPA), phenol (Ph), 4–methylphenol (4–MP), and 4–*tert*–butyl phenol (4-tBP) were purchased from Tianjing Guangfu Fine Chemical Institute (Tianjing, China). All other reagents were of analytical grade. Milli–Q ultrapure water was used during all the experiments.

Morphology and size of GQDs were obtained by a FEI Tecnai G2 20 transmission electron microscopy (TEM) and an atomic force microscope (AFM) from Molecular Imaging with PicoScan Controller. Fluorescence measurements were carried out with an F-4500 fluorescence spectrophotometer (Hitachi, Japan). UV–vis absorption spectra were recorded on a UV–2900 ultraviolet spectrophotometer (Hitachi, Japan). All electrochemical measurements were carried out by a CHI 660D electrochemical workstation (Shanghai, China).

2.2. Preparation of GQDs

GQDs were prepared by a hydrothermal approach. In brief, 20 mg of GO was placed in a Teflon jar at 200 °C for 12 h to obtain reduced GO (rGO), followed by oxidation with a mixture of concentrated HNO_3 (30 mL) and H_2SO_4 (10 mL) under stirring for 24 h and ultrasonication for 24 h at room temperature. The resulting product was diluted with 250 mL ultrapure water and then filtered with a 0.22 μm microporous membrane to remove the residual acids. The filter was redissolved in 40 mL ultrapure water and pH was tuned to 8.0 with NaOH. Finally, the solution was put into a Teflon jar and kept at 200 °C in a Muffle furnace for 24 h. The resulting solution was filtered with a 0.22 μm microporous membrane to remove large particles, and the brown filtrate was collected. The filtrate was further dialyzed 3 times with a dialysis bag (retained molecular weight: 3500 Da). The final products (GQDs) showed blue photoluminescence.

2.3. Preparation of MIPPy/GQDs composite electrode

A glassy carbon (GC) electrode was successively polished using 0.5–0.7 μm and 0.05 μm alumina slurry, followed by rinse with pure water. The GC electrode was further pretreated electrochemically in 0.5 M H_2SO_4 aqueous solution until a stable cyclic voltammogram was obtained. GQDs solution was dropped onto the GC electrode surface and dried at room temperature.

BPA–imprinted polypyrrole was prepared by the electropolymerization of pyrrole on the surface of GQDs modified GC (GQDs/GC) electrode using CV at a potential ranging from −0.2 V to 0.8 V versus a Ag/AgCl reference electrode at a scan rate of 100 mV/s. The prepolymer solution consisted of 0.1 M pyrrole, 20 mM H_2SO_4, and 22 μM BPA as a template. After the electropolymerization, the MIPPy/GQDs composite electrode was repeatedly immersed into methanol–acetic acid (80:2, v/v) solution to remove the template till BPA in the washing solution was not detected by HPLC. Nonimprinted polypyrrole/GQDs (NIPPy/GQDs) composite electrode was prepared as the same procedures except for without the template in the prepolymer solution. The prepared electrodes were kept in 0.1 M PBS (pH 7.0).

2.4. Electrochemical measurements

The electrochemical behaviors of the modified electrodes were evaluated by CV in 10 mM $K_3[Fe(CN)_6]$ solution containing 0.1 M KCl. To quantitatively detect BPA, the MIPPy/GQDs electrode following removing the template was incubated with BPA solution for 210 s and then transferred in the $K_3[Fe(CN)_6]$ solution for DPV measurements, at a scan rate of 50 mV/s and a pulse amplitude of 50 mV and a pulse width of 50 ms. The change value (ΔI_{DPV}) of the peak currents in DPV before and after the incubation was defined as response signal of the sensor. All measurements were made at room temperature. The calibration curve was constructed by plotting ΔI_{DPV} versus BPA concentrations.

2.5. Real samples analysis

Water samples included tap water and sea water which were collected from our laboratory and Xinghai Bay, Dalian, China, respectively. Prior to the measurement, the water samples were filtered with a 0.22 μm membrane to remove large particles. No BPA was detected in the water samples by the HPLC method [28]. Then, the samples were spiked BPA standard solution (40 μM of final concentration) and measured by the DPV method. Recoveries were obtained by the comparison of the concentrations calculated through a calibration curve with the spiked concentration. The spiked sample was also analyzed by a HPLC method [28].

3. Results and discussion

3.1. Preparation and characterization of GQDs

GQDs were synthesized by a facile hydrothermal approach using graphene oxide as original material. The as–prepared GQDs were characterized by AFM and TEM. As shown in Fig. 1, the AFM image showed that the topographic height of the GQDs was 0.7–1.2 nm, suggesting that the GQDs consisted of 1–2 graphene layers, and the horizontal diameter was ~20 nm. GQDs with similar size could be observed in the TEM image though there were some aggregations due to without enough ultrasonication dispersion during the analysis. The GQDs had a broaden absorption band centered at 340 nm and exhibited strong fluorescent emission peaks ranging

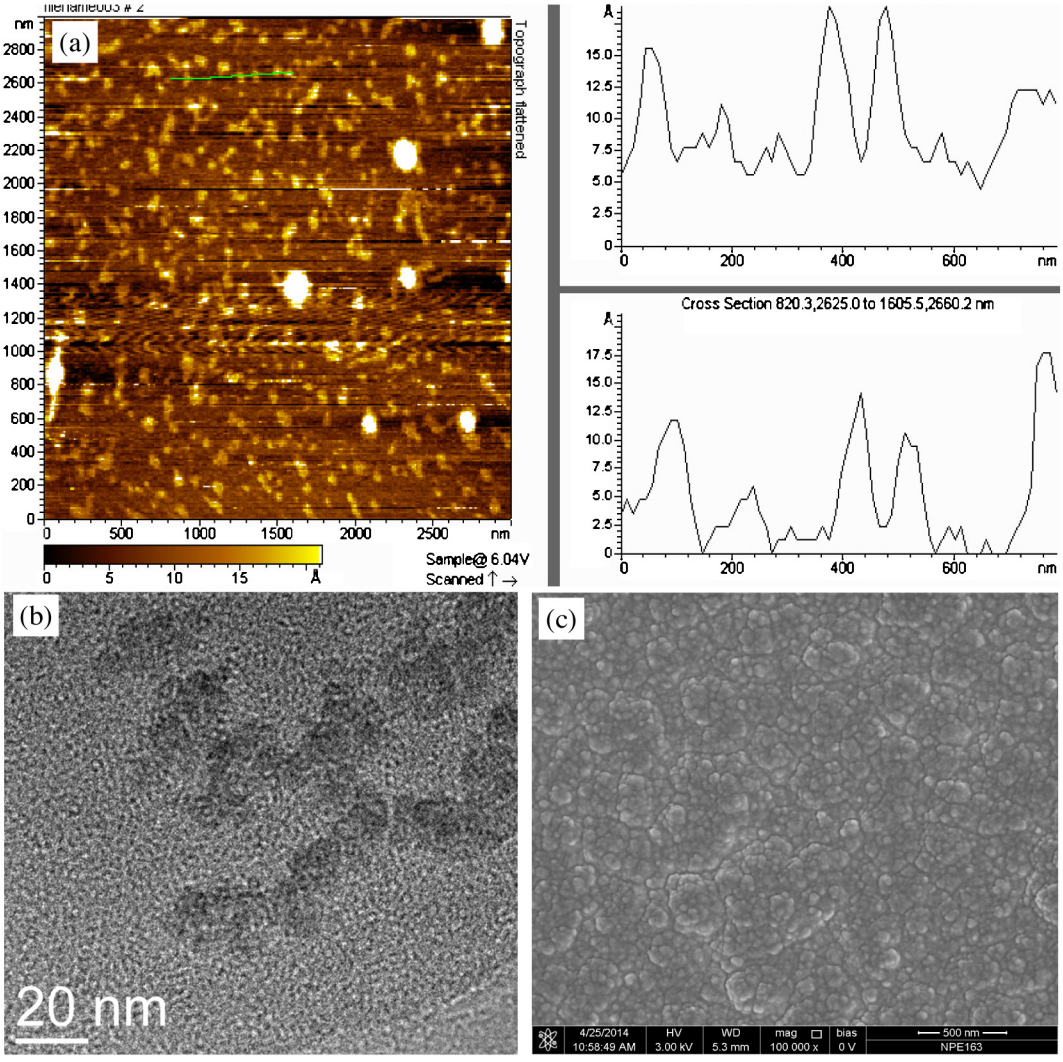

Fig. 1. AFM image (a) and AFM image (b) of the GQDs, and SEM (c) of the MIPPy/GQDs composite on a GC electrode.

from 370 nm to 420 nm depending on the excitation wavelengths (Fig. S1 and Fig. S2). The strongest emission peak was achieved at 420 nm under 320 nm UV excitation. FTIR spectrum (Fig. S3) showed that there was an intense band at ~3450 cm^{-1}, which was assigned to the O—H stretching vibration of C—OH groups. The peaks at 1640 cm^{-1} and 1255 cm^{-1} were attributed to the stretching vibration of C=C and C—O—C [29]. The peak at 1400 cm^{-1} was attributed to the skeletal vibration from graphene domain.

3.2. Preparation of MIPPy/GQDs composite electrode

To prepare MIPPy/GQDs composite electrode, GQDs were firstly loaded on a GC electrode, followed by carrying out the electropolymerization of pyrrole by CV with BPA as a template. Fig. 2 shows cyclic voltammograms of the electropolymerization in presence and absence of the template. In presence of the template, an oxidation peak at 0.48 V was observed at the first scan cycle; while the peak disappeared and the electropolymerization currents decreased in successive CV cycles (Fig. 2a). The peak was attributed to the oxidation of BPA during the electropolymerization. The resulting oxidized products attached on the GQDs/GC electrode, resulting in passivation of the electrode and thus decreasing electropolymerization currents. In absence of the template, the electropolymerization currents gradually increased with increasing number of CV cycles (Fig. 2b). The polymerization process led

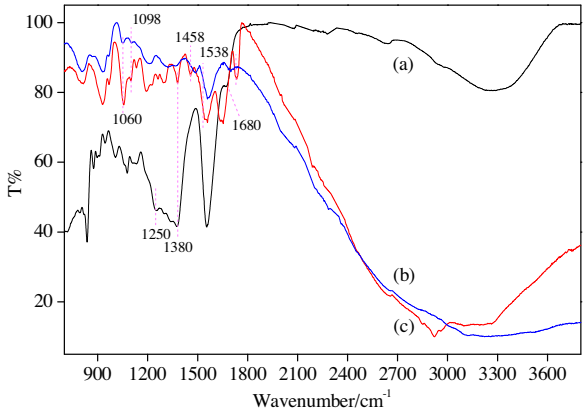

Fig. 2. FTIR spectra of GQDs(a), PPy (b), and MIPPy/GQDs (c).

to the embedment of BPA in the MIPPy/GQDs composite, and then BPA-imprinted sites were obtained following the washing. Fig. 1c shows SEM image of the MIPPy/GQDs composite on a GC electrode. It can be seen that a uniform nanocomposite layer was formed by the electropolymerization. FTIR analysis of PPY, GQDs, and MIPPy/GQDs on ITO substrate was carried out. As shown in Fig. 2, peaks at 1538 cm^{-1}, 1458 cm^{-1} are associated with C—C,

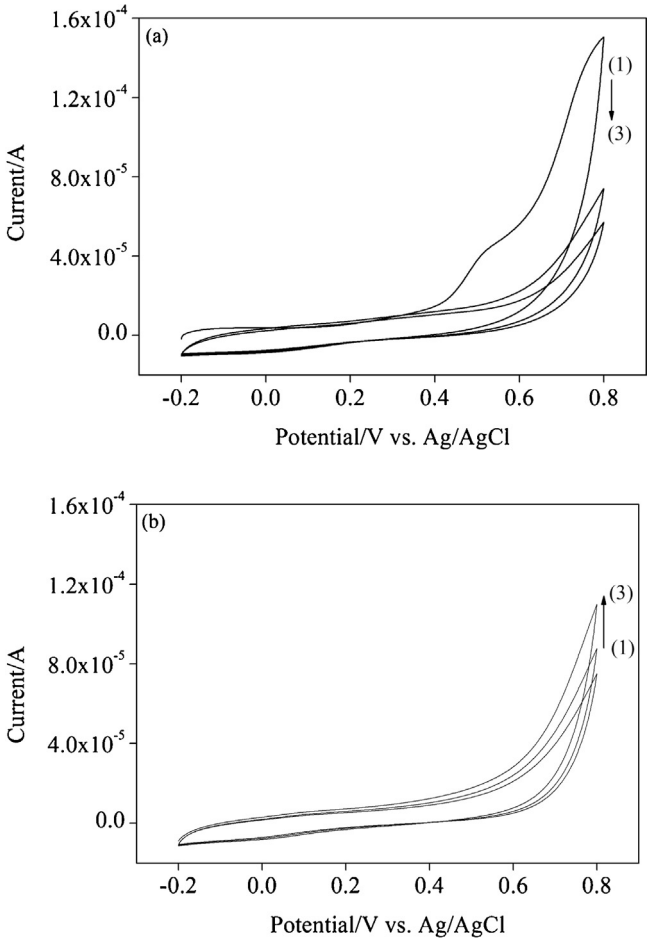

Fig. 3. Cyclic voltammograms for the electropolymerization of 100 mM pyrrole at GQDS/GC electrode in presence (a) and absence (b) of 5 mM BPA in 20 mM H_2SO_4, at a scan rate: 100 mV/S.

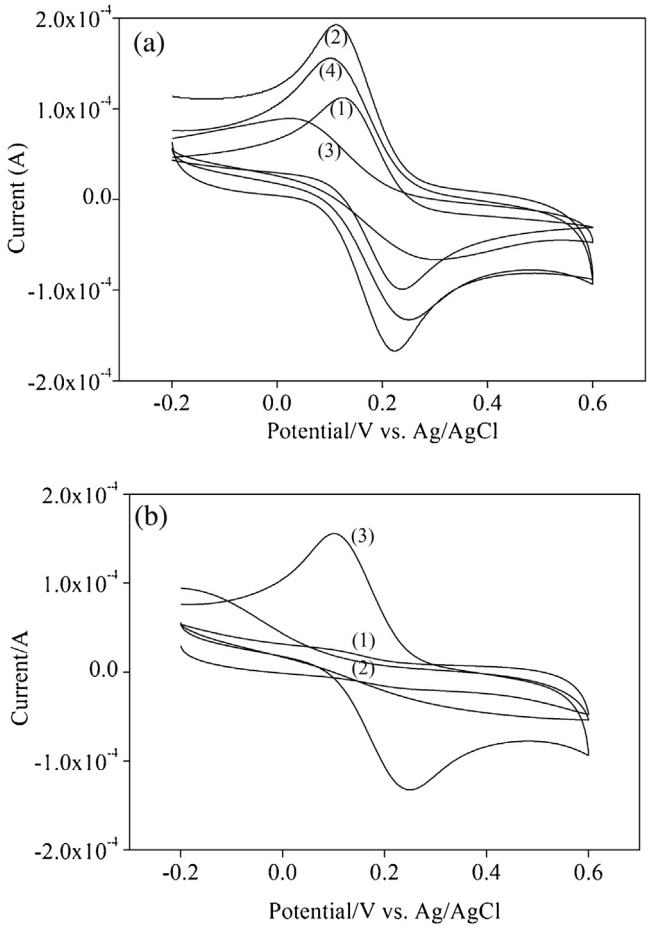

Fig. 4. Cyclic voltammograms of 10 mM $K_3[Fe(CN)_6]$ solution containing 0.1 M KCl at different electrodes. (a): (1) bare GC electrode, (2) GQDs/GC electrode, (3) NIPPy/GQDs electrode, (4) MIPPy/GQDs electrode after the template removal; (b): (1) the MIPPy/GQDs electrode following incubation with 100 μM of the template (1), the MIPPy/GQDs electrode before (2) and after (3) the template removal.

C—N stretching vibration in PPy ring, and peaks at 1676 cm^{-1}, 1380 cm^{-1}, and 1250 cm^{-1} were observed in GQDs, which are attributed to vibration of C=C, C—H, and C—O [30,31]. These characteristics peaks of PPy and GQDs were simultaneously found in MIPPy/GQDs. This fact indicated that the MIPPy/GQDs composite was formed on GC electrode by the electropolymerization. (Fig. 3).

3.3. Electrochemical behavior of modified electrodes

The electrochemical characteristics in stepwise fabrication process of the MIPPy/GQDs electrode were studied by CV with 10 mM $K_3[Fe(CN)_6]$ probe solution. Fig. 4a shows cyclic voltammograms of the probe solution at bare GC, GQDs/GC, MIPPy/GQDs, and NIPPy/GQDs electrodes. A couple of redox peaks were found at bare GC electrode (curve 1), with a peak potential difference (ΔE_p) of 113 mV. The peak current observably increased following the GQDs modification, i.e., GQDs/GC electrode. And both the anodic and cathodic peak potentials (E_p) shifted toward more negative direction and ΔE_p decreased to 110 mV. The shift of E_p and the decrease of ΔE_p were attributed to the fact that the QGDs had higher electron transfer rate and electrical conductivity compared to GC electrode. When polypyrrole was prepared on the GQDs/GC electrode by the electropolymerization in absence of the template, i.e., NIPPy/GQDs electrode, the peaks became poor and peak current decreased and ΔE_p increased to 275 mV. (curve 3). This was because that the polypyrrole, i.e., NIPPy, had lower electron transfer rate and electrical conductivity compared to GQDs and limited the diffusion of $K_3[Fe(CN)_6]$ at the NIPPy/GQDs. Curve 4 shows cyclic voltammogram of the MIPPy/GQDs electrode after the template removal. A pair of large redox peaks was observed, with a ΔEp of 149 mV. The peak current was larger than that at the bare GC and NIPPy/GQDs electrodes but smaller than that at the GQDs/GC electrode. The large peak current could be interpreted by the fact that the imprinted sites in the MIPPy/GQDs composite improved the diffusion of $K_3[Fe(CN)_6]$ at the MIPPy/GQDs electrode.

Curve 1 in Fig. 4b shows the cyclic voltammograms of 10 mM $K_3[Fe(CN)_6]$ at the MIPPy/GQDs electrode following the incubation with the template. No redox peaks of $K_3[Fe(CN)_6]$ were observed, which is similar to the cyclic voltammogram at the MIPPy/GQDs electrode before the template removal (curve 2). This fact indicated that the imprinted sites in the MIPPy/GQDs composite could reabsorb BPA in solution during the incubation, decreasing the diffusion of $K_3[Fe(CN)_6]$ at the MIPPy/GQDs electrode.

The electrochemical impedance (EI) spectroscopy is an effective tool for charactering electrode modifications. In Nyquist plot of EI spectrum, the semicircle part at higher frequencies corresponds to an electron-transfer-limited process while the linear part at lower frequencies indicates a diffusion-controlled process. The semicircle diameter equals to the resistance of the electron-transfer process, which is related to the dielectric and insulating features at the electrode/solution interface [32]. Fig. 5 shows EI spectra of 10 mM $K_3[Fe(CN)_6]$ containing 0.1 M KCl at GC electrode, GQDs/GC electrode, and MIPPy/GQDs electrode before and after the

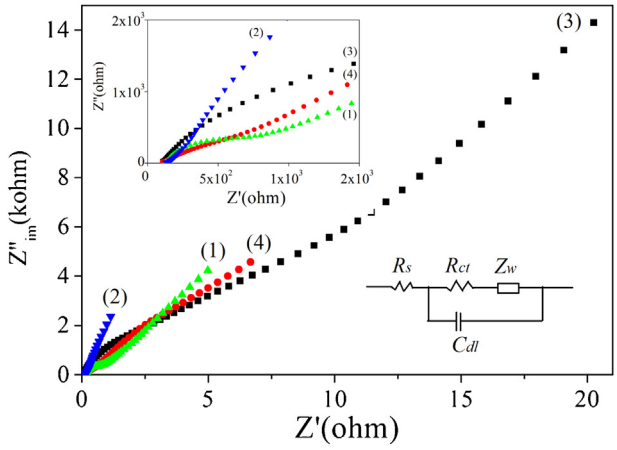

Fig. 5. Electrochemical impedance spectra of 10 mM $K_3[Fe(CN)_6]$ at different electrodes. (1) GC electrode, (2) GQDs/GC electrode, and MIPPy/GQDs electrode (3) before and (4) after the template removal. R_s is solution resistance, R_{ct} is charge transfer resistance, C_{dl} is double layer capacitance, and Z_w is Warburg impedance. The frequency ranging from 1 Hz to 10^5 Hz with signal amplitude of 5 mV.

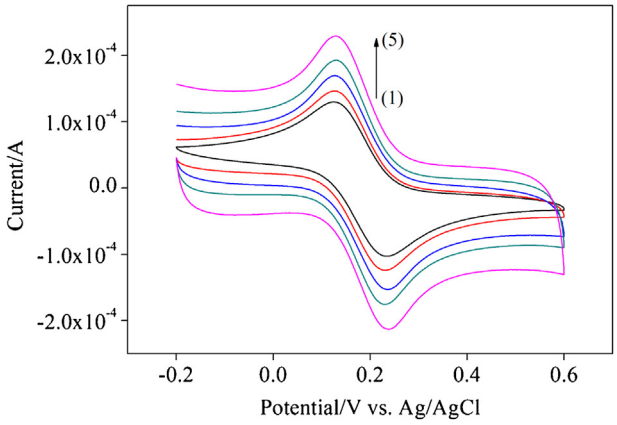

Fig. 6. Effect of the GQDs amount on cyclic voltammograms of 10 mM $K_3[Fe(CN)_6]$ at the MIPPy/GQDs electrode. (1)–(5): 3 μL, 6 μL, 9 μL, 12 μL,15 μL. Scan rate: 100 mV/S.

template removal. The impedance data was analyzed by a Randles circuit (the insert in figure). It can be seen that a small semicircle (750 Ω) at higher frequencies was observed at the GC electrode (curve 1) while only a straight line was recorded at the GQDs/GC electrode (curve 2), indicating that the reaction was controlled by a diffusion-controlled process [32]. There was a large semicircle (7.5 kΩ) at the MIPPy/GQDs electrode before the template removal while the semicircle decreased to 550 Ω when the template was removed by the washing (curve 4). These results further support the fact that the template embedded during the electropolymerization resulted in passivation of the electrode while the imprinted sites exposed by the washing enhanced the diffusion of $K_3[Fe(CN)_6]$ at the MIPPy/GQDs composite and made it easier for electron transfer to take place.

3.4. Optimization of conditions

To prepare the MIPPy/GQDs electrode, GQDs were firstly used to modify a GC electrode due to its large electron transfer rate and good electrical conductivity. Effect of GQDs amount changing from 3 μL to 20 μL on the peak currents of $K_3[Fe(CN)_6]$ was studied. As shown in Fig. 6, the peak currents continually increased with the increase of GQDs amount. The increase was attributed to the continual increase of effective area in the GQD/GC electrode upon the

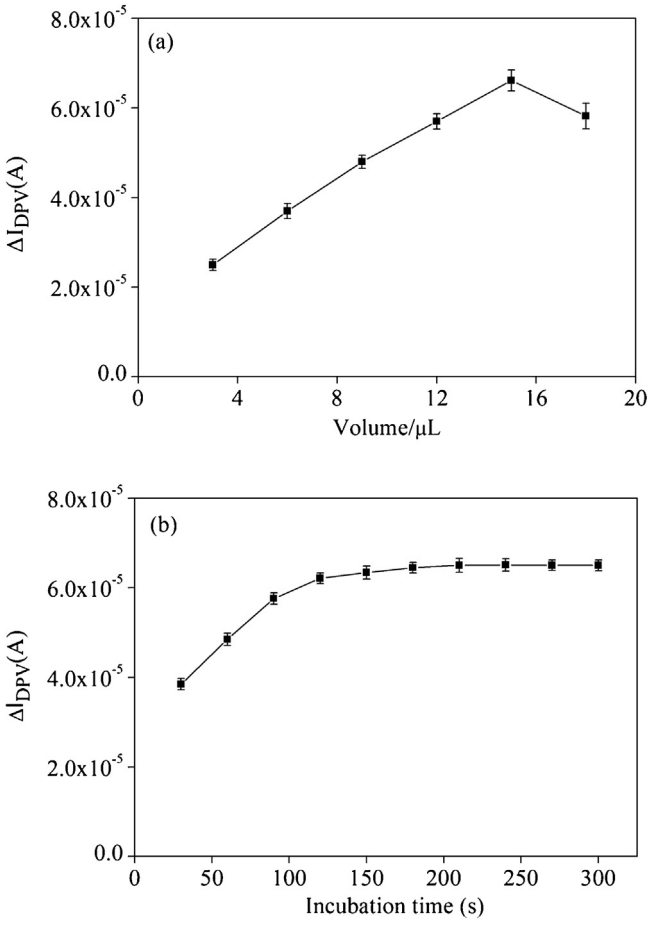

Fig. 7. Effect of the polymerization cycles (a) and incubation time (b) on the response (ΔI_{DPV}) of BPA at the MIPPy/GQDs electrode. 10 mM $K_3[Fe(CN)_6]$ containing 0.1 M KCl.

modification. When the GQDs/GC amount was larger than 15 μL, the peak currents occasionally reduced in successive measurements, which may be due to falling off of GQDs from the electrode surface during the measurement. Thus, 15 μL of GQDs solution was used to modify the GC electrode.

Thickness of the imprinted polymer has an influence on the amount of BPA-imprinted sites, which is related to the polymerization cycles. The thicker the imprinted polymer was, the more the imprinted sites were. However, if the polymer was too thick, it was difficult to completely remove the template from the polymer matrix. Moreover, BPA in solutions could not arrive to the imprinted sites at the deep inner place due to a high mass–transfer resistance, resulting in poor site accessibility and slow binding kinetics. We investigated effect of the polymerization cycles ranging from 3 to 15 cycles on the response value (ΔI_{DPV}). As shown in Fig. 7a, ΔI_{DPV} continually increased and reached a maximum value at 15 cycles. Further increasing the cycles resulted in decrease of ΔI_{DPV}. This decrease may be that excessive cycles increased the transfer resistance of $K_3[Fe(CN)_6]$ at the MIPPy/GQDs electrode. Therefore, 15CV cycles were used in the development of the MIPPy/GQDs electrode.

Effect of the incubation time ranging from 30 s to 300 s on ΔI_{DPV} was investigated. As shown in Fig. 7b, ΔI_{DPV} rapidly increased with the incubation time varying from 30 s to 120 s. Further increasing the incubation time led to a slow increase till a constant value was obtained at 210 s. This fact indicated that the imprinted sites were completely occupied by BPA in solution. To obtain the highest sensitivity, the MIPPy/GQDs electrode was incubated with BPA solution for 210 s for DPV measurements. Since DPV measurement could be

Table 1
Determination of BPA spiked sea water and plastic bottled drinking water by the proposed method and HPLC (n = 3).

Samples	Original	Added (μM)	Detected (μM)	Recoveries (%)	RSD(%)	Recoveries (%) by HPLC
Sea water	nd	30.0	28.1	93.7%	3.54%	95.7%
Bottled water	nd	30.0	28.4	94.5%	1.66%	96.3%

nd: no detected by the proposed method.

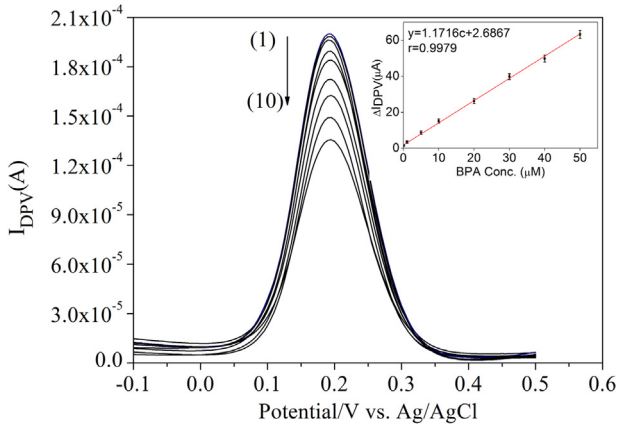

Fig. 8. DPV curves of 10 mM $K_3[Fe(CN)_6]$ at the MIPPy/GQDs electrode after incubation with different concentration BPA solutions. (1)–(10): 0, 0.1 μM, 1 μM, 5 μM, 10 μM, 20 μM, 30 μM, 40 μM, and 50 μM. The inset in fig is a calibration curve between ΔI_{DPV} value versus BPA concentrations.

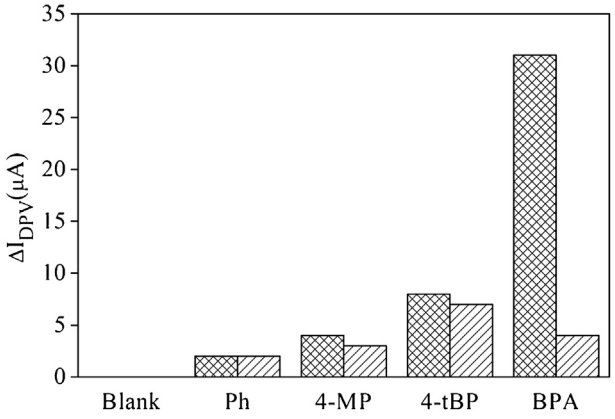

Fig. 9. The response (ΔI_{DPV})of the MIPPy/GQDs (gridding) and NIPPy/GQDs (diagonal) electrodes to different compounds (20 μM). The MIPPy/GQDs and NIPPy/GQDs electrodes were incubated with the compounds, follow by carrying out DPV measurements in 10 mM $K_3[Fe(CN)_6]$ containing 0.1 M KCl.

completed within 12 s under the optimized parameters, the whole analysis time for the detection of BPA was less than 4 min.

3.5. Analytical characteristics

DPV was used to quantitatively detect BPA in solutions. The analytical performance of the sensor was evaluated by measuring the response (ΔI_{DPV}) of the sensor when the MIPPy/GQDs electrode was incubated with different concentration BPA solutions under the optimized conditions. There was a linear relationship between BPA concentrations varying from 0.1 μM to 50 μM and ΔI_{DPV} value, as shown in Fig. 8. The resulting calibration equation was $\Delta I_{DPV} = 1.1716c + 2.6867$ (r = 0.9979). The limit of detection (LOD) was 0.04 μM (S/N = 3), which was 50 times lower than the standard value (0.01 mg/L, 2.28 μM) for drinking water quality of China (GB 5749-2006), and lower than some previous results by electrochemical sensors based on molecularly imprinted polymer, such as 0.1 μM [33], 420 μM [34], 0.06 μM [35], 0.138 μM [36].

The reproducibility of the sensor was evaluated for repeated measurements of 20 μM BPA aqueous solution. The sensor was washed with the methanol–acetic acid (80:2, v/v) solution for 5 min after each measurement. The relative standard derivation (RSD) was 2.2%, showing good reproducibility and regeneration ability. To evaluate the stability of the sensor, the fresh sensor was kept for 15 days in PBS (pH 7.0) at 4 °C, and the response signal of the sensor kept 95% of original signal, showing good long–term stability. Good reproducibility and stability of the present sensor were attributed to the good stability of the MIPPy/GQDs composite and the reversibly binding of the imprinted sites to BPA; more important, the detection process did not involve oxidization reaction of BPA and thus avoided the passivation of the MIPPy/GQDs electrode.

3.6. Selectivity of the sensor

Selective recognition of the template was an important merit for a sensor based on molecularly imprinted polymer. Here Ph, 4-MP, and 4-tBP with phenol structure were used to check selectivity of the present sensor. As show in Fig. 9, the response (ΔI_{DPV}) of BPA at the MIPPy/GQDs electrode was 15.5, 7.7 and 3.9 times more than that of Ph, 4-MP and 4-tBP (20 μM for each compound), respectively, indicating that the sensor could selectively detect BPA in the presence of other phenolic compounds. In additional, the imprinting effect was evaluated by the comparison between the MIPPy/GQDs and NIPPy/GQDs electrodes. It can be seen that the NIPPy/GQDs electrode had smaller responses for BPA and other compounds compared to the MIPPy/GQDs electrode, and the calculated imprinted factor (the ration of ΔI_{DPV} between the MIPPy/GQDs electrode and the NIPPy/GQDs electrode to BPA) is 7.8.

3.7. Analysis of real water samples

To evaluate the suitability of the present sensor for practical applications, the sensor was applied to detect BPA in tap water and sea water. The water samples collected were simply centrifuged to remove any large suspended particles. The initial detection by HPLC showed there was no presence of BPA in the samples. In this case, the water samples were spiked with 30 μM BPA standard solution and were subjected to DPV measurements by the sensor. The achieved recoveries were 94.5% and 93.7% for the tap and sea water samples, respectively, as shown in Table 1. The same samples were analyzed by a HPLC method. There was no significant difference between the proposed method and HPLC method by a paired *t*-test analysis with SPSS software ($p < 0.05$). These results indicated the potential suitability of the sensor for the quantification of BPA in real waters.

4. Conclusions

In conclusion, we developed a novel electrochemical sensor based on the MIPPy/GQDs composite electrode for the detection of BPA in water samples. The MIPPy/GQDs composite could specifically recognize BPA in aqueous solutions, which resulted in the decrease of the peak currents of $K_3[Fe(CN)_6]$ at the MIPPy/GQDs composite electrode in DPV. The achieved LOD was 0.04 μM. High

sensitivity was attributed to high electron transfer rate and good electrical conductivity of GQDs while good selectivity was derived from the BPA-imprinted sites in the MIPPy/GQDs composite. The proposed sensor showed good repeatability and stability. All in all, the proposed method provides a powerful platform for rapid (less than 4 min) and sensitive analysis of BPA in water samples.

Acknowledgements

The work was supported by the Basic Research Program of Key Laboratory, Education Department of Liaoning Province, China (No. LZ2014008), National Natural Science Foundation of China (No. 21407019), and Opening Foundation of Key Laboratory of Industrial Ecology and Environmental Engineering (MOE).

Appendix A. Supplementary data

Supplementary data associated with this article can be found, in the online version, at http://dx.doi.org/10.1016/j.snb.2016.04.146.

References

[1] A.M. Calafat, Z. Kuklenyik, J.A. Reidy, S.P. Caudill, J. Ekong, L.L. Needham, Urinary concentrations of bisphenol A and 4-nonylphenol in a human reference population, Environ. Health Perspect. 113 (2005) 391–395.
[2] I.A. Lang, T.S. Galloway, A. Scarlett, W.E. Henley, M. Depledge, R.B. Wallace, et al., Association of urinary bisphenol A concentration with medical disorders and laboratory abnormalities in adults, Jama-J. Am. Med. Assoc. 300 (2008) 1303–1310.
[3] M. Rezaee, Y. Yamini, S. Shariati, A. Esrafili, M. Shamsipur, Dispersive liquid–liquid microextraction combined with high-performance liquid chromatography-UV detection as a very simple, rapid and sensitive method for the determination of bisphenol A in water samples, J. Chromatogr. A 1216 (2009) 1511–1514.
[4] A. Garcia-Prieto, M. Loreto Lunar, S. Rubio, D. Perez-Bendito, Determination of urinary bisphenol A by coacervative microextraction and liquid chromatography-fluorescence detection, Anal. Chim. Acta 630 (2008) 19–27.
[5] E. Herrero-Hernandez, R. Carabias-Martinez, E. Rodriguez-Gonzalo, Use of a bisphenol-A imprinted polymer as a selective sorbent for the determination of phenols and phenoxyacids in honey by liquid chromatography with diode array and tandem mass spectrometric detection, Anal. Chim. Acta 650 (2009) 195–201.
[6] G. Provencher, R. Berube, P. Dumas, J.F. Bienvenu, E. Gaudreau, P. Belanger, et al., Determination of bisphenol A, triclosan and their metabolites in human urine using isotope-dilution liquid chromatography–tandem mass spectrometry, J. Chromatogr. A 1348 (2014) 97–104.
[7] S.R. Yazdinezhad, A. Ballesteros-Gomez, L. Lunar, S. Rubio, Single-step extraction and cleanup of bisphenol A in soft drinks by hemimicellar magnetic solid phase extraction prior to liquid chromatography/tandem mass spectrometry, Anal. Chim. Acta 778 (2013) 31–37.
[8] Y. Deceuninck, E. Bichon, S. Durand, N. Bemrah, Z. Zendong, M.L. Morvan, et al., Development and validation of a specific and sensitive gas chromatography tandem mass spectrometry method for the determination of bisphenol A residues in a large set of food items, J. Chromatogr. A 1362 (2014) 241–249.
[9] M. Kawaguchi, R. Ito, N. Endo, N. Okanouchi, N. Sakui, K. Saito, et al., Liquid phase microextraction with in situ derivatization for measurement of bisphenol A in river water sample by gas chromatography–mass spectrometry, J. Chromatogr. A 1110 (2006) 1–5.
[10] A. Ozcan, Synergistic effect of lithium perchlorate and sodium hydroxide in the preparation of electrochemically treated pencil graphite electrodes for selective and sensitive bisphenol a detection in water samples, Electroanalysis 26 (2014) 1631–1639.
[11] Y. Zhu, C.Q. Zhou, X.P. Yan, Y. Yan, Q. Wang, Aptamer-functionalized nanoporous gold film for high-performance direct electrochemical detection of bisphenol A in human serum, Anal. Chim. Acta 883 (2015) 81–89.
[12] Y. Jiao, K. Sung-Eun, C. Misuk, Y. Ik-Keun, C. Woo-Seok, L. Youngkwan, Highly sensitive and selective determination of bisphenol-A using peptide-modified gold electrode, Biosens. Bioelectron. 61 (2014) 38–44.
[13] W.Y. Chen, L.P. Mei, J.J. Feng, T. Yuan, A.J. Wang, H.Y. Yu, Electrochemical determination of bisphenol A with a glassy carbon electrode modified with gold nanodendrites, Microchim. Acta 182 (2015) 703–709.
[14] B. Lu, M. Liu, H. Shi, X. Huang, G. Zhao, A novel photoelectrochemical sensor for bisphenol a with high sensitivity and selectivity based on surface molecularly imprinted polypyrrole modified TiO_2 nanotubes, Electroanalysis 25 (2013) 771–779.
[15] X. Xin, S. Sun, H. Li, M. Wang, R. Jia, Electrochemical bisphenol A sensor based on core-shell multiwalled carbon nanotubes/graphene oxide nanoribbons, Sens. Actuators B 209 (2015) 275–280.
[16] L. Zhou, J. Wang, D. Li, Y. Li, An electrochemical aptasensor based on gold nanoparticles dotted graphene modified glassy carbon electrode for label-free detection of bisphenol A in milk samples, Food Chem. 162 (2014) 34–40.
[17] L.-J. Kou, R.-N. Liang, X.-W. Wang, Y. Chen, W. Qin, Potentiometric sensor for determination of neutral bisphenol A using a molecularly imprinted polymer as a receptor, Anal Bioanal. Chem. 405 (2013) 4931–4936.
[18] M.-H. Piao, H.-B. Noh, M.A. Rahman, M.-S. Won, Y.-B. Shim, Label-free detection of bisphenol A using a potentiometric immunosensor, Electroanalysis 20 (2008) 30–37.
[19] B. Kang, J.H. Kim, S. Kim, K.-H. Yoo, Aptamer-modified anodized aluminum oxide-based capacitive sensor for the detection of bisphenol A, Appl. Phys. Lett. 98 (2011).
[20] M.A. Rahman, M.J.A. Shiddiky, J.-S. Park, Y.-B. Shim, An impedimetric immunosensor for the label-free detection of bisphenol A, Biosens. Bioelectron. 22 (2007) 2464–2470.
[21] N. Singh, K.K. Reza, M.A. Ali, V.V. Agrawal, A.M. Biradar, Self assembled DC sputtered nanostructured rutile TiO2 platform for bisphenol A detection, Biosens. Bioelectron. 68 (2015) 633–641.
[22] Q. Li, H. Li, G.-F. Du, Z.-H. Xu, Electrochemical detection of bisphenol A mediated by Ru(bpy)(3) (2+) on an ITO electrode, J. Hazard. Mater. 180 (2010) 703–709.
[23] D. Chen, H.B. Feng, J.H. Li, Graphene oxide: preparation, functionalization, and electrochemical applications, Chem. Rev. 112 (2012) 6027–6053.
[24] S.J. Zhu, J.H. Zhang, X. Liu, B. Li, X.F. Wang, S.J. Tang, et al., Graphene quantum dots with controllable surface oxidation, tunable fluorescence and up-conversion emission, RSC Adv. 2 (2012) 2717–2720.
[25] S.J. Zhu, J.H. Zhang, S.J. Tang, C.Y. Qiao, L. Wang, H.Y. Wang, et al., Surface chemistry routes to modulate the photoluminescence of graphene quantum dots: from fluorescence mechanism to up-conversion bioimaging applications, Adv. Funct. Mater. 22 (2012) 4732–4740.
[26] J. Zhao, G.F. Chen, L. Zhu, G.X. Li, Graphene quantum dots-based platform for the fabrication of electrochemical biosensors, Electrochem. Commun. 13 (2011) 31–33.
[27] M. Roushani, Z. Abdi, Novel electrochemical sensor based on graphene quantum dots/riboflavin nanocomposite for the detection of persulfate, Sens. Actuators B 201 (2014) 503–510.
[28] F. Tan, H.X. Zhao, X.N. Li, X. Quan, J.W. Chen, X.M. Xiang, et al., Preparation and evaluation of molecularly imprinted solid-phase microextraction fibers for selective extraction of bisphenol A in complex samples, J. Chromatogr. A 1216 (2009) 5647–5654.
[29] L. Wang, F. Liu, C. Jin, T. Zhang, Q. Yin, Preparation of polypyrrole/graphene nanosheets composites with enhanced thermoelectric properties, RSC Adv. 4 (2014) 46187–46193.
[30] J. Ali, G.-U.-D. Siddiqui, Y.J. Yang, K.T. Lee, K. Um, K.H. Choi, Direct synthesis of graphene quantum dots from multilayer graphene flakes through grinding assisted co-solvent ultrasonication for all-printed resistive switching arrays, RSC Adv. 6 (2016) 5068–5078.
[31] S. Bose, T. Kuila, M.E. Uddin, N.H. Kim, A.K.T. Lau, J.H. Lee, In-situ synthesis and characterization of electrically conductive polypyrrole/graphene nanocomposites, Polymer 51 (2010) 5921–5928.
[32] C. Xie, H. Li, S. Li, J. Wu, Z. Zhang, Surface molecular self-assembly for organophosphate pesticide imprinting in electropolymerized poly(*p*-aminothiophenol) membranes on a gold nanoparticle modified glassy carbon electrode, Anal. Chem. 82 (2010) 241–249.
[33] L.L. Zhu, Y.H. Cao, G.Q. Cao, Electrochemical sensor based on magnetic molecularly imprinted nanoparticles at surfactant modified magnetic electrode for determination of bisphenol A, Biosens. Bioelectron. 54 (2014) 258–261.
[34] D.C. Apodaca, R.B. Pernites, R. Ponnapati, F.R. Del Mundo, R.C. Advincula, Electropolymerized molecularly imprinted polymer film: eis sensing of bisphenol A, Macromolecules 44 (2011) 6669–6682.
[35] P.H. Deng, Z.F. Xu, J.H. Li, Y.F. Kuang, Acetylene black paste electrode modified with a molecularly imprinted chitosan film for the detection of bisphenol A, Microchim. Acta 180 (2013) 861–869.
[36] J.D. Huang, X.M. Zhang, S. Liu, Q. Lin, X.R. He, X.R. Xing, et al., Electrochemical sensor for bisphenol A detection based on molecularly imprinted polymers and gold nanoparticles, J. App. Electrochem. 41 (2011) 1323–1328.

Biographies

Feng Tan received his Ph.D. in Analytical Chemistry from Dalian Institute of Chemical Physics, Chinese Academy of Sciences in 2005. Now he is an associate professor at Dalian University of Technology, China. His research interest focuses on functional materials synthesis and its' application in sensing of toxic substances.

Longchao Cong is a M.S. candidate in Environmental Engineering at Dalian University of Technology, China. His current research interest focuses on biosensors.

Xiaona Li received her Ph.D. in Environmental Engineering from Dalian University of Technology, China. Now she is a senior engineer at Dalian University of Technology. Her research interest is pollution control.

Qian Zhao received his M.Sc. in Environmental Engineering in 2014 from Dalian University of Technology, China. His research interest focuses on electrochemical sensor.

Hongxia Zhao received her Ph.D. from Dalian Institute of Chemical Physics, Chinese Academy of Sciences in 2006. Now she is an associate professor at Dalian University of Technology, China. Her research interest is trace analysis, environmental fate of emergent toxic substances.

Xie Quan received his Ph.D. in 2000 at University of Graz, Austria. In 1997. He was appointed a full professor in Dalian University of Technology, China. In 2005, he was appointed as Changjiang Scholar distinguished Professor by Chinese Ministry of Education and a winner of the National Science Fund for Distinguished Young Scholars. His interests include water pollution control, environmental monitoring, and environmental material applications.

Jingwen Chen received his Ph.D. in Environmental Chemistry from Nanjing University, China in 1997. In 2001, he was promoted to be a full professor. In 2013, he was appointed as Changjiang Scholar distinguished Professor by Chinese Ministry of Education and a winner of the National Science Fund for Distinguished Young Scholars. His current interests include pollution eco-chemistry, computational and ecological toxicology.